NON-DESTRUCTIVE EVALUATION (NDE) OF BOND LINE USING CARBON NANOFIBER AND NANOTUBE MODIFIED FILM ADHESIVE AND INFRARED THERMOGRAPHY

William W. Taylor, Nazim Uddin, Melike Dizbay-Onat, Kuang-Ting Hsiao*
University of South Alabama
Mobile, Alabama, United States of America

ABSTRACT

A film adhesive is commonly used to form the bond line between composite or metal parts. The bond line's quality and performance can be affected by defects such as voids, impurities, agglomerations, and other structural issues found within it; in addition, defects can form due to damage or delamination. Identifying these defects is possible with non-destructive evaluation (NDE). In this paper, the joule-heating effect through carbon nanofibers (CNF) and carbon nanotubes (CNT) modified film adhesive will be used along with infrared thermography for bond line defect inspection. Due to the difference in the electrical conductivity between the modified epoxy and the defect, joule heating can cause a different temperature at the defect; thus, in theory, the defect can be viewed by infrared thermography. The percentage of carbon nanofiller in a film adhesive changes the measurement quality due to its relationship to electrical conductivity. An Acrylonitrile Butadiene Styrene (ABS) equilateral triangle defect with 30 mm sides was used inside bond line samples. These bond lines were composed of epoxy and nanofillers of CNF and CNT at various concentrations. Each concentration was evaluated individually and bonded onto two single-ply CFRP coupons. In this study, the feasibility of using carbon nanofillers of different concentrations as a medium for identifying and characterizing defects through NDE infrared thermography was investigated and validated the effectiveness of this new NDE approach. In the future, aligning nanofiller for bond lines could be a potential research direction to improve upon what this study strives to achieve.

Keywords: Bond Line, CFRP, Film Adhesive, NDE, Defect, Carbon Nanofiber, Carbon Nanotube, Through-Thickness Conductivity, Infrared Thermography

*Corresponding author: Kuang-Ting Hsiao, Email: kthsiao@southalabama.edu

1. INTRODUCTION

Adhesive bonded joints surpass their usual counterparts in the performance such as fatigue resistance, strength to weight ratio, and overall damage tolerance, and have been implemented throughout the aerospace, automotive, sports, and many other industries in an increasing trend over the years [1]. NDE allows detection of defects on the interior of composite materials or the bond line without destroying the composite structure. Infrared thermography is a common type of NDE technique to evaluate thin composite panel for defects. The defect displays a distinct heat signature when an external heat source such as a flashlight radiates the heat flux onto the composite panel. This method is useful for detecting defects across a large area and is done without coming into

contact with the part making it easier to implement [2]. The reflected temperature signature coming into the infrared camera allows a view of structural defects such as voids, agglomerations, and delamination of ply-layers within composites. This is due to the differences in thermal conductivity between the defect and the composite part [3].

For this study, carbon fiber reinforced polymer (CFRP) coupons were bonded together with a range of weight percentages of carbon nanofibers (CNF) and carbon nanotubes (CNT) embedded into an epoxy matrix along with an intentional defect. Instead of a typical external heat source used in traditional infrared thermography NDE, in this novel approach, an internal electrical heating source was induced by applying constant voltage into the conductive CNT/CNF modified bond line area. Note that the CNF/CNT modified bond line can also increase the mechanical strength of the bond line [4, 5]; hence, the CNF/CNT modified bond line can have multifunctional purposes as well. This electrical heating effect of the CNT/CNF modified epoxy bond line comes from joule heating when the electrical current passes through the region. Having a composite with a higher through-thickness electrical conductivity (Tt.E.C.) could be used to create a lightweight, yet very conductive, composite to combat lightning strike damage on the exterior of an aircraft [6].

Joule heating has been reported for curing epoxy composite adhesives paired with very electrically conductive materials such as bucky paper (very thin sheets made of multi-walled carbon nanotubes (MWCNT)) and achieved a 67% improvement in bonding strength over cured pure epoxy [7]. As stated in the literature, the typical CFRP Tt.E.C. is at a range of $10^{-3} - 10^{0}$ S/m [8] since the epoxy is non-conductive at a range of $2.3\text{x}10^{-8}$ S/m [6]. Individual CNFs have a measured electrical conductivity of roughly 10^{5} S/m [9] and individual CNTs at a range of $10^{4} - 10^{7}$ S/m [10]. In this experimental study, to ensure the most current permeates through the bonded CFRP testing samples, highly electrically conductive metals, aluminum, and copper were used as electrodes to connect to the single-lap bonded CFRP samples. Aluminum and copper have the electrical conductivity of $3.5\text{x}10^{7}$ S/m and $5.3\text{x}10^{7}$ S/m, respectively [11].

The magnitude of electrical conductivity in a CNT/CNF modified film adhesive is dictated in part to the concentration of conductive nanofillers within it. This is known as percolation theory. In composites, the percolation trend tends to follow a power rule function while in logarithmic scale. In other words, the composite has low conductivity at low concentrations then sharply rises as more is added before tapering off at a high conductivity [12]. The concentration of conductive nanofillers where the electrical conductivity of the composite begins to dramatically increase is known as the percolation threshold and is different for every kind of nanofiller [12]. The nearly linear relationship between the percolation threshold and the tapering off point is known as the percolation zone.

2. EXPERIMENTATION

2.1 Materials and Instruments

The materials used in this experiment include PR-24-XT-HHT grade carbon nanofiber (CNF) (Pyrograph Products/Applied Sciences, Inc.), Graphistrength CS1-25 carbon nanotube (CNT) (Arkema Group), T700S unidirectional fabric (680 g/m^2 areal weight, 12k tow size, and 1.8 g/cm^3 fiber density, Toray), Epikure-W curing agent and Epon 862 epoxy resin (mixing ratio 26.5:100) (Miller-Stephenson Chemical Co. Inc.), surfactants S-191 and S-192 (BYK), 120 grit, 320, 400

grit, wet 800 grit 3M sandpapers, half-hard 110 copper sheet metal, and Hillman 6063-T5 aluminum sheet metal.

The hardware used to evaluate and record data for this experiment included a Flickr E40 thermal infrared camera, a 210W GW Instek PSP-603 power supply, and an Agilent 34405A 5 $\frac{1}{2}$ Digits Multimeter.

2.2 Methods

2.2.1 Through-Thickness Electrical Conductivity Film Adhesive Study

The through-thickness electrical conductivity (Tt.E.C.) of resin infused with varying amounts of conductive nanofillers was investigated to understand the electrical conductivity increase due to CNT and CNF, as well as their percolation trend. The minimum concentration used was 1 wt% nanofillers for this test (i.e., resin tray test) and 0.8 wt% for the CFRP bond line tests (which was due to a nanofiller mixing ratio calculation mistake). The resistance and geometry of the resin sample must be known to find out the Tt.E.C.. For CNT/epoxy film conductivity, the geometry was constrained by creating a 3D printed housing for the resin's electrical resistance to be measured (Figure 1). The material used was ABS as it had a glass transition temperature of approximately $105\,^{o}\mathrm{C}$ [13] and became malleable at higher temperatures but did not melt until reaching at least $200^{o}\mathrm{C}$ [14]. This meant it could hold a sample of resin and then directly cure at $120\,^{o}\mathrm{C}$ for 2 h without deforming much with the internal structures in place such as the two copper plates acting as the electrodes. The copper sheet was cut into roughly one square inch pieces and sanded with 220 grit sandpaper. The copper sheet was fitted into the bottom entrance and the top, sitting on the ABS ridge separating both from touching. The Epon 862 epoxy resin infused with various weights of CNT, mixed with an appropriate amount of Epikure-W curing agent, was poured into the bottom sheet and covered with the top sheet. The bottom and top ABS trays had small holes exposing the back side of the copper sheets which allowed the multimeter's probes to read the resistance of the resin sample sandwiched between the two electrodes. The sample was cured in a $120\,^{o}\mathrm{C}$ vacuum oven for two hours until cured. The sample was cooled afterwards for about 5 min and then measured for its resistance at the room temperature ($22^{o}C$). By this assessment, 1 wt%, 2 wt%, 3 wt%, and 4 wt% CNT and CNF at the same concentrations were chosen to be the bond line nanofillers for the thermographic NDE defect testing based on the electrical conductivity found. The next section will address the detailed process of mixing the nanofibers (CNT and CNF), the Epon 862 epoxy, Epikure-W curing agent, and the surfactants, as well as the film adhesive manufacturing process.

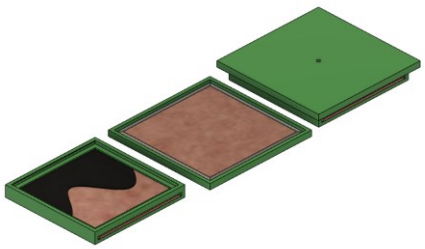

Figure 1: Resin resistance evaluation test (Rr.E.T.) comprised the bottom resin tray, top resin tray, and the completed assembly (left to right).

2.2.2 Resin Film Adhesive Preparation

To create the film adhesives used in testing, only one main process was needed for both CNF and CNT. The only difference in preparing these nanofillers into film adhesive was that the CNT was submerged in a rationed amount of Epon 862 overnight in a vacuum oven at 90 ºC. The CNT came in the form of pellets at room temperature, which already had its CNT (about 25wt% concentration) well dispersed in the solid bisphenol-A epoxy. As shown in Figure 2, both CNT and CNF based film adhesives followed the rest of the process once the first round of high shear mixing (HSM) occurred. The manufacturing of CNF-based film adhesives started by measuring out one-part Epon 862 and 0.265 parts of Epikure-W by weight. Then the surfactants S191 and S192 were rationed to the same weight fraction of CNF (i.e., 4.0wt%). The CNF-Epon 862 batch was manually mixed to minimize the CNF clumps. After the mixture appeared roughly homogeneous, it was placed onto a hotplate at 90 ºC and high shear mixed (HSM) with an industrial stirring machine for one hour at about 300 RMP. The direction of rotation was switched at 30 mins for even mixing. Then, a sample was taken for quality assessment using the Nikon Eclipse LV150 microscope. The quality of the batch was checked after sonication concluded and if the dispersion seemed adequate the batch would undergo dilution. Portions of the 4 wt% CNF batch were set aside and mixed with a rationed amount of Epon 862 to create 0.8 wt%, 2 wt%, and 3 wt% batches. The dilution process was performed the same for both nanofillers. Finally, 30 g of each batch poured into a proper amount of Epikure-W and hand mixed to complete the resin blends. After mixing, the beakers were put through the B-stage process and had their temperature and their cure cycle monitored. The B-staging operation finished at about 35-40 min at 120 ºC. Once the batches reached B-stage, they were poured onto a sheet of parchment paper on a hotplate of about 60-70 ºC. The parchment paper was put under a metal sheet raised off the hot plate with metal shims to create a roughly consistent film thickness (0.30-0.60 mm). Finally, after passing through the gap, the CNF film adhesive is created.

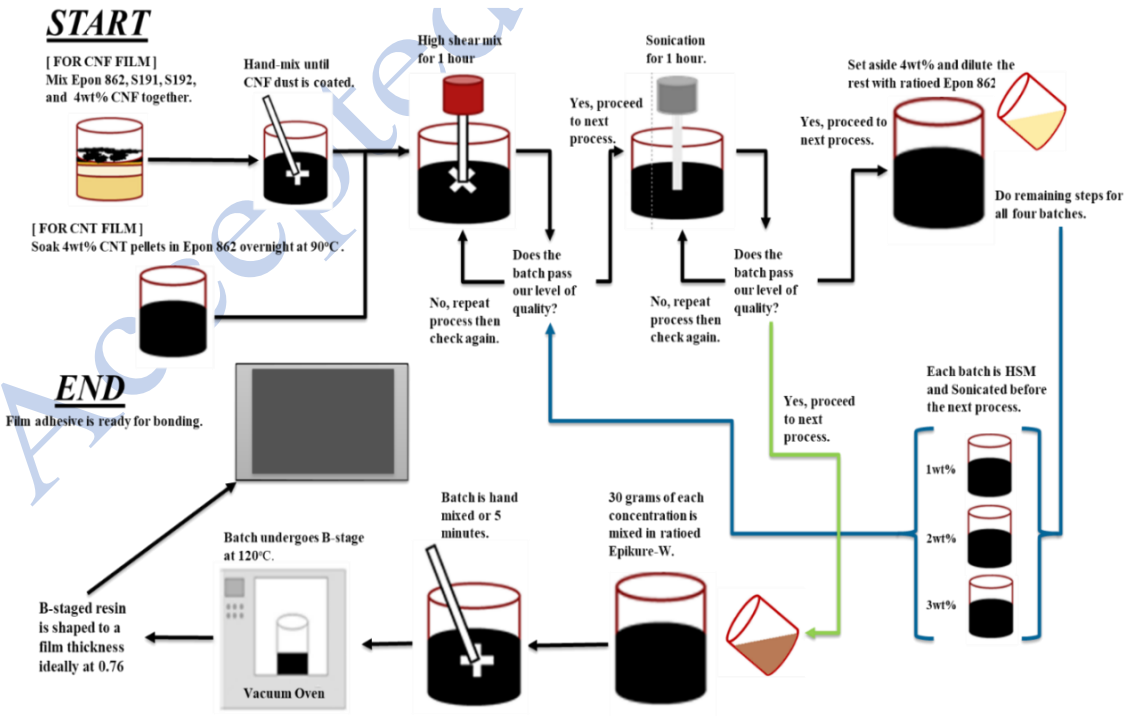

Figure 2: Carbon nanofiller film adhesive manufacturing process.

2.2.3 CFRP Coupon Preparation

T700S unidirectional carbon fiber fabric was cut into an 18 x 6-inch rectangle with the unidirectional fiber parallel to the 6-inch length. 30 g of control epoxy resin was created by mixing 1-part Epon 862 to 0.265 parts Epikure-W curing agent, then hand mixed for 5 min, alternating directions occasionally. The resin was then impregnated into the carbon fiber fabric using a resin roller. The resin impregnated fabric was placed onto a 120 ^{o}C industrial hot press for 25-30 min. to reach B-stage and form the prepreg. The prepreg was taken from the oven and laid to cool for 15 min at the room temperature.

The prepreg was cut into six pieces and placed on the Out of Autoclave Vacuum Bag Only (OOA-VBO) setup (Figure 3) to be further cured into six single layer CFRP panels. The prepreg was first vacuumed to -86 KPa and then was placed into the 120 ^{o}C hot press for two hours to cure and then demolded (Figure 4). After the OOA-VBO process, the single layer CFRP coupons were sanded down on both sides with 120, 320, 400, and wet 800 grit sandpaper until the surfaces were smooth to the touch. This threshold of smoothness was reached at roughly 0.60 mm thickness, starting from the CFRP thickness of roughly 0.65-0.7 mm. After the sanding process, the coupons were placed in a soap-water bath to remove dusts from sanding and then dried in an oven at 90 ^{o}C for 5 min. They then were left to cool at room temperature for another 5 min. A light wash of acetone on the coupons was applied and completed the CFRP coupon preparation.

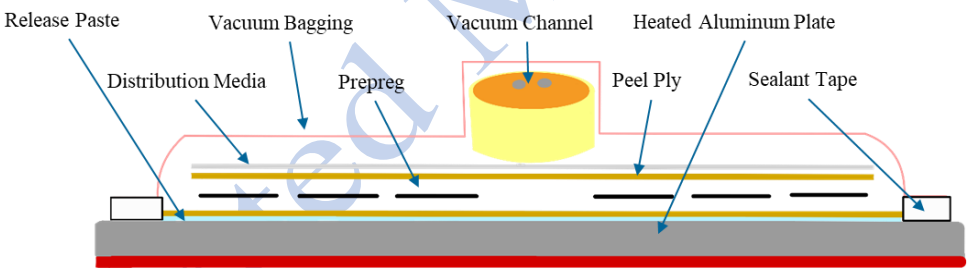

Figure 3: OOA-VBO layout.

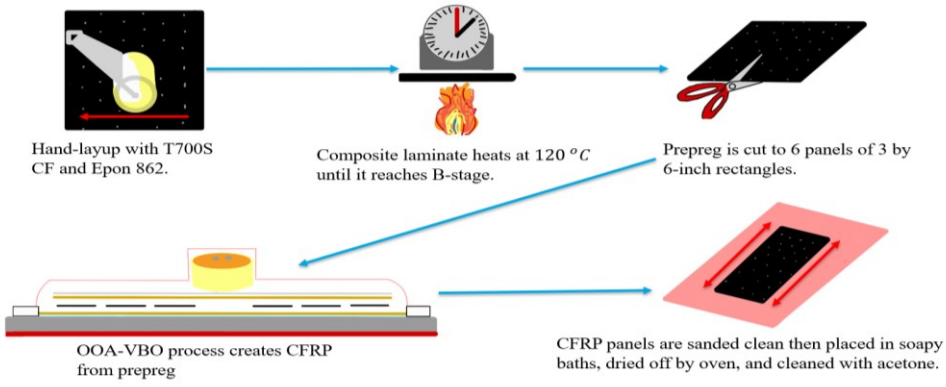

Figure 4: CFRP coupon manufacturing process.

2.2.4 Sample Preparation and Bonding

The film adhesive and the CFRP panels were brought together to create the testing sample (Figure 5). This was started by measuring out a 76.2 mm x 76.2 mm (3 x 3-inch) square onto the film adhesive's parchment paper layer then cut out the square shape film adhesive. A 3D printed ABS triangle punch card was used to make an indentation of a triangle with 30 mm sides. If a film adhesive were too sticky due to insufficient B-stage treatment, it would be placed into the freezer at $-17\ ^{o}C$ for at least 10 seconds to become rigid to the touch. If the film adhesive were too thin to meet the height of the ABS defect (0.76mm after sanding with 400 grit sandpaper) an additional layer of film adhesive would be added on top. The indentation was scrapped off carefully using a thumbtack to leave a triangular void with a clean CFRP surface surrounded by the film adhesive. Once completed, the ABS triangle defects were inserted. The back of the CFRP coupon was marked where the defect sat on the other side. The top CFRP panel was rolled/pressed carefully from side to side to limit the amount of air trapped inside while bonding. Then, the testing samples were put into a vacuum oven at $120\ ^{o}C$ for two hours. Once the curing process concluded, the edges and sides of the test samples were sanded and polished following the same cleansing process as for cleaning the CFRP coupons. By doing this, the voltage applied, ideally, will only create current cross through the bond line in the thickness direction rather than finding any other bypath. Prior to testing, the ends of the CFRP samples are sanded gently with 220 grit sandpaper to remove any epoxy coating and cleaned with acetone to reduce any surface contact resistance. The bonding setup is shown in Figure 5.

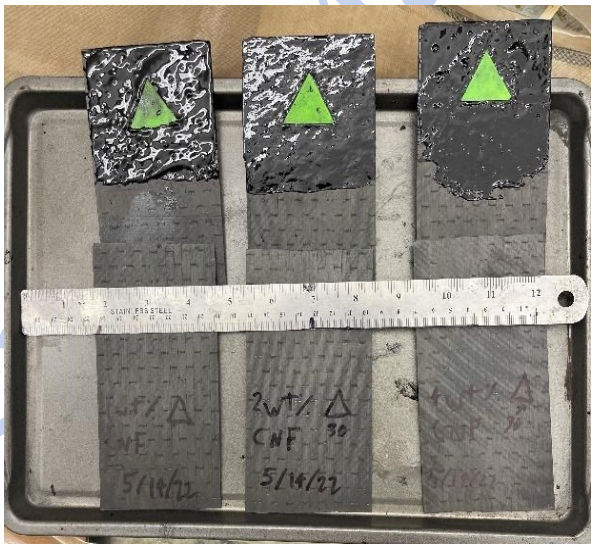

Figure 5: CNF 1 wt% (0.8 wt%), 2 wt%, and 4 wt% ready to bond to the CFRP coupons.

2.2.5 Infrared Thermography Study

The defects within the CFRP film adhesive bond line were evaluated with the thermal infrared camera. The camera was mounted 12 inches away from the testing sample to allow full view of the bonding area. Calibrating the infrared camera (especially the emissivity input) was achieved through monitoring what temperature it was measuring compared to a thermocouple in the same region underneath the sample. Different regions and hot spots on the bond area were measured this way as well to gage the accuracy of the camera. This calibration practice was inspired by

researchers used to determine the emissivity of aluminum AW 6082 for their infrared camera [15]. Vice grips that held the testing sample in place were modified by adding an ABS printed arch to allow the pliers to press firmly onto the aluminum strips (as electrodes) onto the exposed carbon fibers of the CFRP panels. The cables from the power supply were connected onto the two strips of acetone cleaned aluminum sheet metal of around 25.4 mm x 76.2 mm (1 by 3 inches) area with a thickness of 0.77 mm. As the ABS defect was nonconductive, the electrical current could not pass through it. Instead, the electrical current went through the bond line which invoked joule heating. From this difference in electrical conductivity, in theory, the defect should be shown as a colder region compared with the rest of bonded area and can be recorded with the infrared camera. This bond line infrared thermography NDE experimental setting is shown in Figure 6.

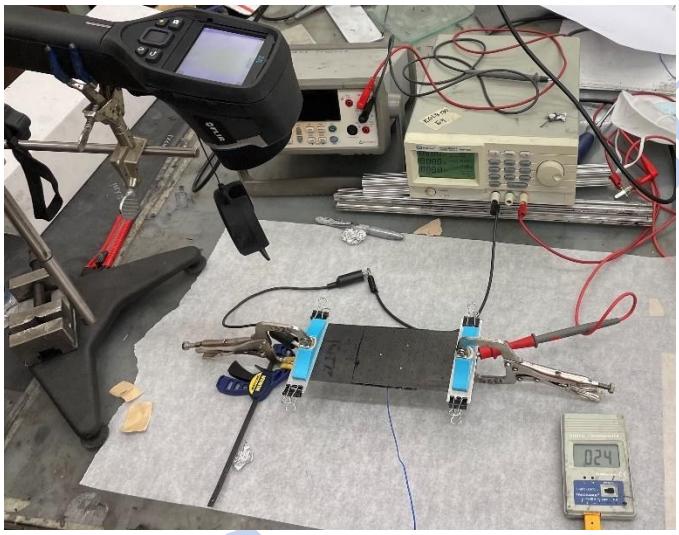

Figure 6: Infrared thermography testing setup.

As shown in Figure 6, the camera pointed directly onto the center of the triangle spot indicated by the markings given before bonding. The emissivity was found to close to a blackbody (1.0), due to the dark and low reflectivity of the CFRP testing sample, which gave the closest measurements with the thermocouple that measured between $1 - 2\ ^{o}C$ colder.

3. RESULTS

3.1 Film Adhesive Tray Electrical Conductivity Measurements

The through-thickness electrical conductivity measured from the CNT/resin mixture cured in the tray setup and the CNT/resin bond line setup had a loose correlation to each other despite the same nanofiller concentrations (Figure 7). The tray study showed a weaker Tt.E.C. than that from the CFRP bond line test samples. This can be from a variety of reasons such as: uneven bond line thickness, partial cover of the film adhesive onto the copper panels in the tray prior to curing, resin shrinkage, or resin seeping into the probe terminals inside the tray obscuring the exposed copper plate prior to curing. All of these reasons would impact the overall Tt.E.C. measurements, especially the tray study/setup. The electrical resistance (R), the bond line area (A), and thickness of the bond (t) of the sample were recorded. The electrical conductivity of the material was calculated using this mathematical relationship:

$$\sigma = \frac{t}{R*A} \qquad (\frac{S}{m}) \qquad [1]$$

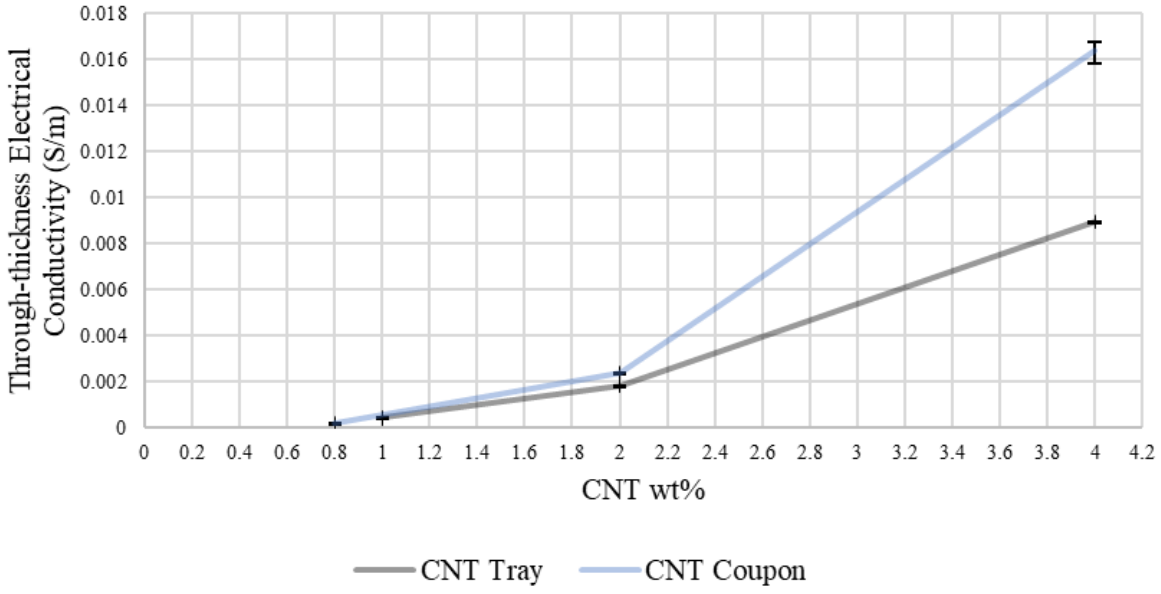

Figure: 7: Comparison of the Tt.E.C. measurements from the CNT tray shown in Figure 1 to the CFRP/CNT-bond line samples in Figure 5 and Figure 6.

3.2 Infrared Thermography Imaging

Determining the scale of visual quality of the defects was considered after a comparison of all images. The following grading scale has been used to determine the visual quality of the defect image shown in the infrared thermography imaging analysis below.

1. *Triangular area visible: Edges and points are clearly visible.*
2. *Triangular area visible: Clear edges, fuzzy points.*
3. *Obscured visibility: Fuzzy edges and points.*
4. *Hotspots: Cold areas have a semblance to defect.*
5. *Hotspots: Cold area has no semblance to defect.*
6. *No temperature change throughout the bond line area.*

Figure 8.c and Figure 9.d show the clearest images of infrared thermography results for the CNF/epoxy bond line NDE tests and CNT/epoxy bond line tests, respectively. Table 1 describes the raw data collected from the infrared thermography testing. A constant voltage of 5 V was imposed onto every sample and continuously recorded for about 1 min. duration. The CNF samples proved troublesome to read based on uneven bond lines, and exposed resin outside the bond line,

which formed after curing the test sample. All of these reasons could cause non-uniform joule-heating across the bond line and produced an irregular temperature signature.

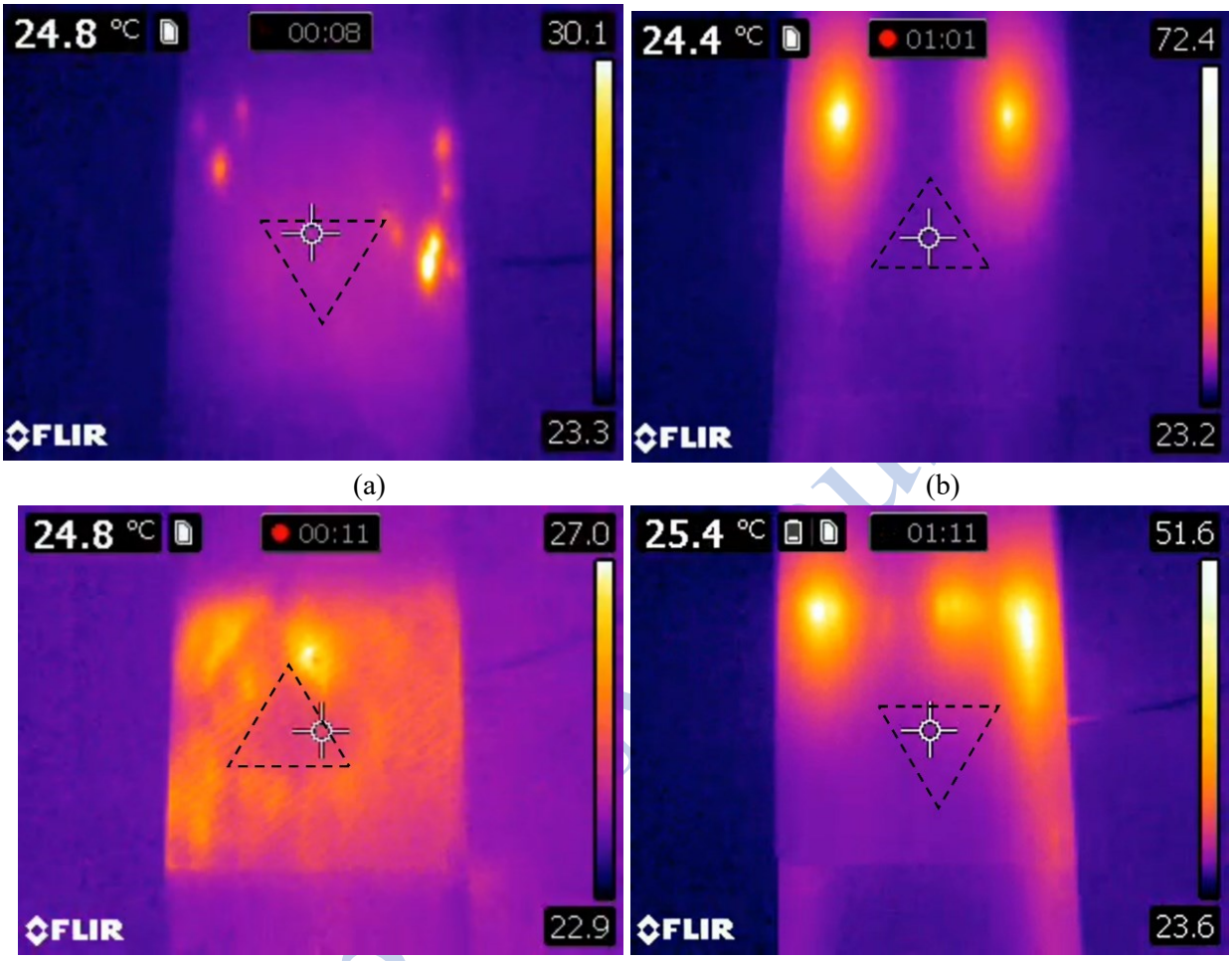

Figure 8: The CNF samples taken at the point of clearest image. The range of temperature for when the defect displayed most clearly was from $22.9 - 72.4\ ^{o}C$, a 49.5-degree difference. The room temperature was roughly $22\ ^{o}C$. A constant voltage of 5 V was applied to all samples. (a) 0.8 wt% CNF, (b) 2 wt% CNF, (c) 3 wt% CNF, (d) 4 wt% CNF.

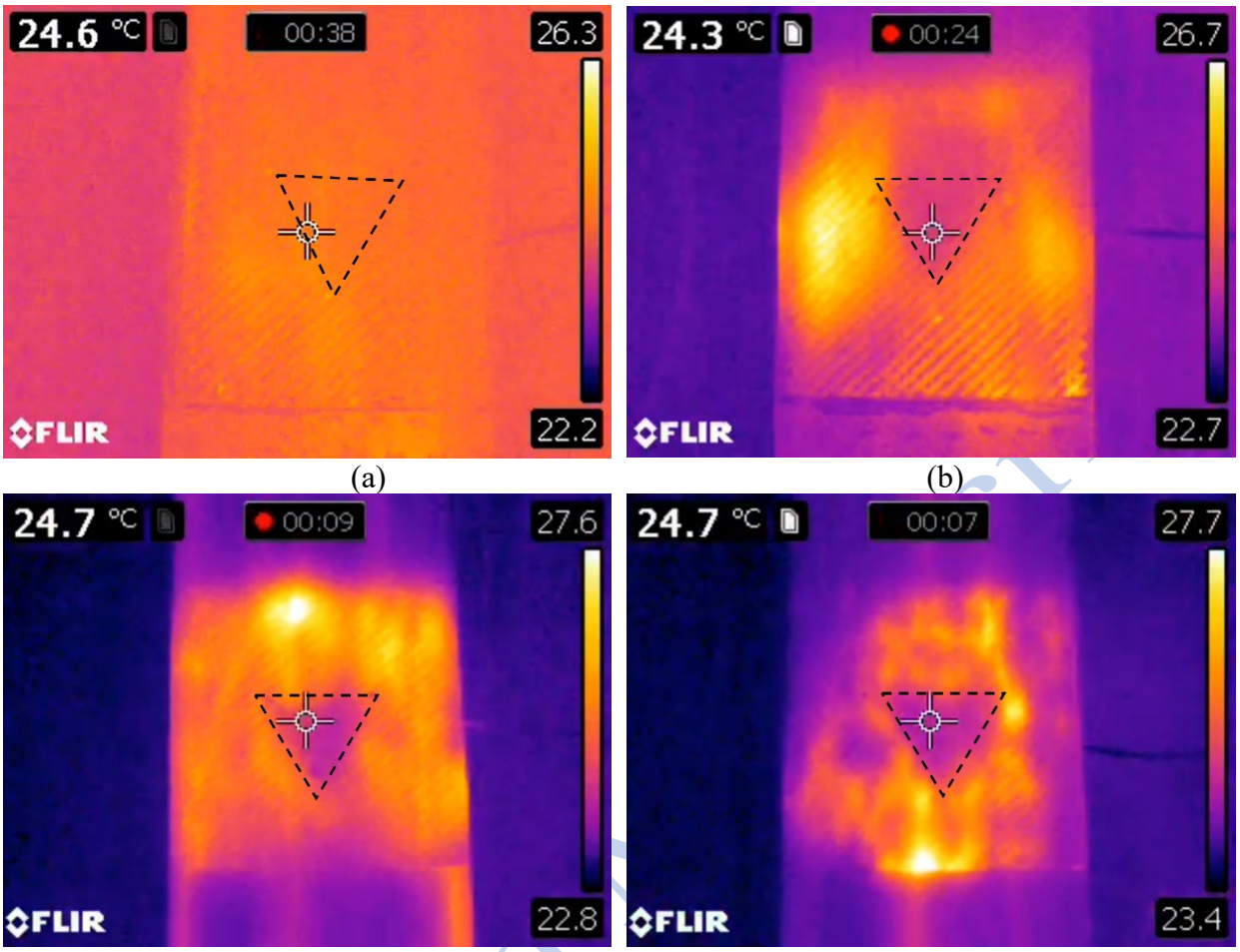

Figure 9: The CNT samples taken at the point of clearest image. The range of temperature for when the defect displayed most clearly was $22.2 - 27.7\ ^{o}C$, a 5.5-degree difference. The room temperature was roughly $22\ ^{o}C$. A constant voltage of 5 V was applied to all samples. (a) 0.8 wt% CNT, (c) 2 wt% CNT, (c) 3 wt% CNT, (d) 4 wt% CNT.

Table 1: Infrared Thermography Testing Results.

Case	Average Resistance (Ohm)	Voltage (V)	Current (Amps)	Power (W)	Visual Quality From 6 to 1 (1 is the best)	Time of Clearest Image
0.8 wt% CNF	77.52	5	0.760	0.3	5	0:08
2 wt% CNF	21.89	5	0.266	1.3	4	1:01
3 wt% CNF	18.27	5	0.294	1.4	2	0:11
4 wt% CNF	12.47	5	0.444	2.2	5	1:11
0.8 wt% CNT	792.12	5	0.008	0.040	6	0:38
2 wt% CNT	49.93	5	0.165	0.8	3	0:24
3 wt% CNT	7.51	5	0.849	4.2	2	0:09
4 wt% CNT	7.62	5	1.0	4.9	1	0:07

The CNT samples were receptive to the tests as they had a more balanced through-thickness with a standard deviation of 0.000102 m compared to CNF's 0.00361 m, a 3.5 multiplicative difference. Table 2 touches on key data from the study with the total % improvement, average bonding area, and average Tt.E.C. for each sample. Notice how the COV of the Tt.E.C. increases dramatically near the percolation threshold. Every measure of resistance from the bond line was combined with its average thickness and bond area and then once more averaged resulting in the Tt.E.C. values below.

Table 2: Testing Sample Dimensions and Tt.E.C. Improvement for various CNT, CNF Concentrations.

Film Adhesive Type	**Weight Percent (wt%)**	**Average Bonding Area (m^2)**	**Average Bond line Thickness (mm)**	**Average Tt.E.C. (S/m)**	**COV of Tt.E.C. (%)**	**Improvement over 0.8wt%'s Respective Nanofiller**	**Improvement of all samples over the 0.8wt% CNF sample Tt.E.C.**
CNT	0.8	5.50E-03	0.885	2.03E-04	0.0%	0%	-87.39%
	2	5.93E-03	0.701	2.37E-03	0.6%	1064.33%	47.20%
	3	5.69E-03	0.914	2.14E-02	5.0%	10434.56%	1229.19%
	4	6.05E-03	0.754	1.64E-02	2.5%	7948.33%	918.63%
CNF	0.8	5.78E-03	0.723	1.61E-03	0.5%	0%	0.00%
	2	5.82E-03	0.87	6.83E-03	1.8%	323.18%	324.22%
	3	5.65E-03	0.889	8.62E-03	1.1%	434.08%	435.40%
	4	5.33E-03	0.794	1.20E-02	2.9%	641.03%	645.34%

Although not investigated in this preliminary experimental study, after comparing all the results, it was felt that an improved visual image could be created with the use of z-aligned film adhesive (epoxy matrix with carbon nanofillers aligned in the z-direction) used in making the CNF Z-threaded CFRP (ZT-CFRP) prepreg. Note that unidirectional ZT-CFRP laminates compared with the traditional CFRP laminate's Tt.E.C were found as 16.24 S/m vs 0.161 S/m, respectively (a 9,987% enhancement) [16]. In addition, the ZT-CFRP laminate has significantly higher through-thickness thermal conductivity of 9.85 W/m-K compared with traditional CFRP's 1.31 W/m-K (about 7.5 times higher) [17] . Another benefit of using z-aligned film as the film adhesive to bond ZT-CFRP laminates, in terms of only NDE concerns, could be reducing the apparent stretching of the defect image due to the unidirectional carbon fiber.

3.3 Through-Thickness Electrical Conductivity (Tt.E.C.) Percolation Trend

The CNT trend appears to follow the general trend of the percolation relationship with respect to the weight concentration. The percolation threshold appears to be at 2 wt% for CNT and at 0.8 wt% for CNF (Figure 10). This could be due to the dimensions of the nanofillers where the CNF has a diameter of roughly 100 nm and lengths of 50 – 200 μm [18] and the CNT used in this study

has a diameter ~ 10- 15 nm and length ~ 0.1-10 μm [19]. This difference in size can explain why more CNT was needed to exceed CNF's electrical conductivity initially. The CNT was shorter and thinner which meant it would have a weak electrically conductive for the structural network at lower concentrations yet much higher at higher concentrations. The apparent electrical conductivity of the CNT is brought out as it passed CNF after it reached its percolation threshold.

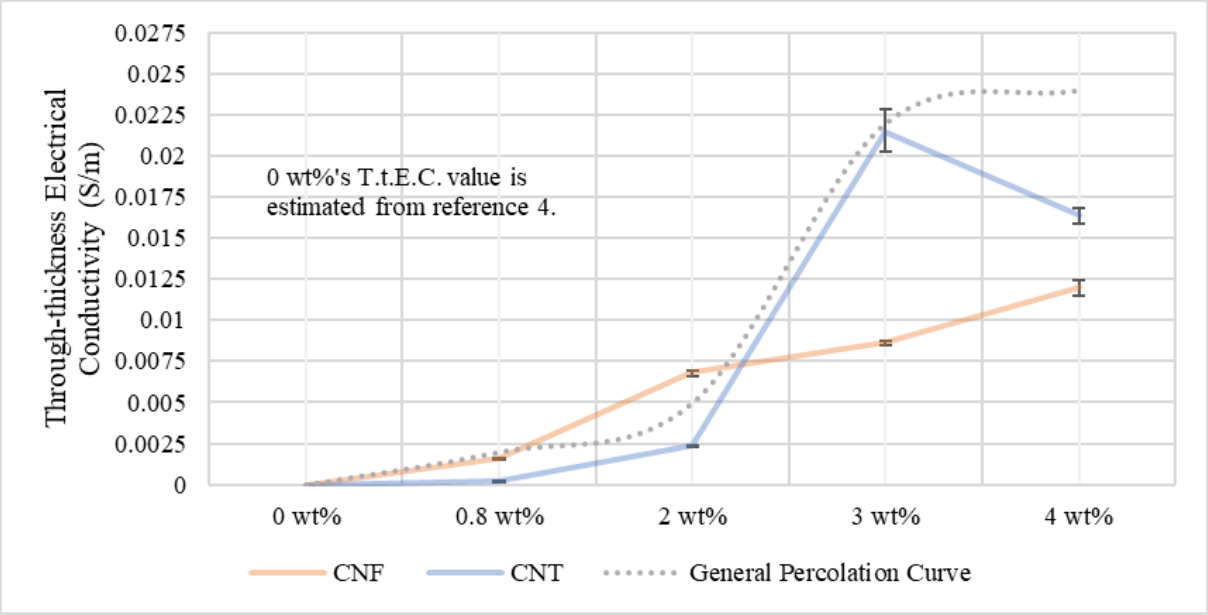

Figure 10: Tt.E.C. comparison between CFRP/CNT-film adhesive bond line tests and CFRP/CNF-film adhesive bond line tests.

CNT had a higher Tt.E.C. compared to CNF as expected. However, 4 wt% CNT dipped in conductivity which went against the general percolation trend. This can be substantiated through the level of difficulty of creating 4 wt% CNT with a dispersion and sonication quality comparable to the lower concentration's improved quality.

By combining the information from Figures 8, 9, and 10, one can find additional insight. The clearest image from the CNF bond line tests was the 3 wt% concentration case (Figure 8). Although it did have a higher conductivity over CNT in this case from the percolation graph (Figure 10), the other samples could not show a definitive defect possibly due to the CFRP coupons having cured resin on the outside of the bonding area facing the camera that could not be removed without damaging the samples. This could cause the electric current to bypass the bond line area entirely and into the top CFRP coupon. This would heat the exposed resin causing it to become very warm and overpower the subtle temperature range needed to view the defect clearly. This suggested the need to remove any bypassing electrical current short-cuts when using this NDE approach. The CNT samples on the other hand did very well in showing the defect (Figure 9) with the clearest image at 4 wt%, although 3 wt% was a close second. The dip in conductivity at 4 wt% shown in Figure 10 can be attributed to the difficulty in producing it due to the increase in viscosity. In fact,

the higher viscosity also caused issues in the high shear mixing stage and the mixing speed needed to be reduced about 300 RPM from the originally planned 600 RPM.

4. CONCLUSIONS AND FUTURE WORK

In this novel nanofiller-modified bond line NDE study, the feasibility and effectiveness of using various concentrations (0.8wt%, 2wt%, 3wt%, 4wt%) of CNF and CNT in the modified epoxy film adhesive to bond traditional unidirectional CFRP plates, whereas the conductive CNT/CNF modified film adhesive served as the internal joule heating source for distinguishing the internal defects with the aid of infrared thermography. With a constant voltage (5 V) being applied, it was found the defects can be identified in the cases of epoxy film adhesive modified with 3wt% CNF, 2wt% CNT, 3wt% CNT, and 4wt% CNT. Note the 3wt% CNT and 4wt% showed very clear and well-defined defect shape that matched the inserted equilateral triangle ABS defect very nicely. The high-fidelity infrared thermography NDE results can also be corelated to the high through-thickness electrical conductivity of the corresponding CNF and CNT modified epoxy film adhesive.

Previous research has already proved that CNF/CNT modified epoxy can enhance the mechanical bonding strength of CFRP laminates. This paper showed the high electrical conductivity of CNF/CNT modified resin can enable a new NDE approach. The CNF/CNT modified adhesive has a strong potential to serve the desired multifunctional purposes in modern adhesive technologies. In the future, it would be interesting to further extend this study to aligned CNF/CNT in the modified film adhesive and use CNF/CNT z-threaded CFRP (ZT-CFRP) to replace traditional CFRP since the two materials can significantly increase the through-thickness electrical conductivity and the through-thickness thermal conductivity by many folds thus. Thus, it likely can lead to a notable enhancement of fidelity, accuracy, thermal signature penetration depth, and resolution of this new CNF/CNT modified resin CFRP bond line NDE approach. In addition to the enhanced NDE performance, the additional improvement in mechanical strength can also be expected. The bond line NDE between CFRP or ZT-CFRP with metal or dissimilar materials will be also considered for future investigation.

5. ACKNOWLEDGMENT

The authors acknowledged the financial support by the National Science Foundation (Award number: 2044513) and Alabama Department of Commerce through the Alabama Innovation Fund (Award number: 150436). The authors are grateful for the carbon fiber materials provided by Toray, the CNT/epoxy masterbatch provided by Arkema, and the surfactants provided by BYK USA, Inc.

6. REFERENCES

1. Budhe, S., Banea, M. D., De Barros, S. & Da Silva, L. F. M., “An updated review of adhesively bonded joints in composite materials.” *International Journal of Adhesion and Adhesives*, 72 (2017): 30-42.

2. Gholizadeh, S., "A review of non-destructive testing methods of composite materials." *Procedia Structural Integrity*, 1 (2016): 50-57. https://doi.org/10.1016/j.prostr.2016.02.008.
3. Usamentiaga, R., Venegas, P., Guerediaga, J., Vega, L., Molleda, J. & Bulnes, F. G.. "Infrared thermography for temperature measurement and non-destructive testing." *Sensors*, 14, no. 7 (2014): 12305-12348.
4. Hsiao, K.T., Alms, J. & Advani, S., "Use of epoxy/multiwalled carbon nanotubes as adhesives to join graphite fibre reinforced polymer composites." *Nanotechnology*,v14 (2003): 791-793.
5. Taylor, W.W., Uddin, M.N., Islam, M.R., Dizbay-Onat, M. & Hsiao, K-T., "A preliminary study of using film adhesives containing aligned and unaligned nanotubes and nanofibers for bonding CFRP laminates and steel plates." *Proceedings of SAMPE 2022 Conference*, Charlotte, NC, USA. May 23-26, 2022.
6. Kumar, V., Yokozeki, T., Karch, C., Hassen, A., Hershey, C., Kim, S., Lindahl, J., Barnes, A., Bandari, Y. & Kunc, V., "Factors affecting direct lightning strike damage to fiber reinforced composites: A review." *Composites Part B: Engineering*, 83 (2020).
7. Sung, P.C. & Chang, S.C., "The adhesive bonding with buckypaper–carbon nanotube/epoxy composite adhesives cured by Joule heating." *Carbon*, 91 (2015): .
8. Kumar, V., Yokozeki, T., Okada, T., Hirano, Y., Goto, T., Takahashi, T. & Ogasawara, T., "Effect of through-thickness electrical conductivity of CFRPs on lightning strike damages." *Composites Part A: Applied Science and Manufacturing*, 114 (2018): 429-438. https://doi.org/10.1016/j.compositesa.2018.09.007.
9. Bal, S., "Experimental study of mechanical and electrical properties of carbon nanofiber/epoxy composites." *Materials & Design* (1980-2015), 31.5 (2010): 2406-2413.
10. Li, C., Thostenson E. T. & Chou T.-W., "Dominant role of tunneling resistance in the electrical conductivity of carbon nanotube–based composites." *Applied Physics*, Letters 91.22 (2007).
11. Bell, T., "What Makes Metals Conductive?". *ThoughtCo.* March 2, 2020. July 19th, 2022 https://www.thoughtco.com/electrical-conductivity-in-metals-2340117.
12. Loos M., "Chapter 5 – Fundamentals of Polymer Matrix Composites Containing CNTs" *Carbon Nanotube Reinforced Composites*, William Andrew, 2015. https://doi.org/10.1016/B978-1-4557-3195-4.00005-9.
13. Rahman M., Schott N. R. & Sadhu L. K.. "Glass transition of ABS in 3D printing" COMSOL Conference, Boston, MA, 2016.
14. Singh, N. & Singh, R., "Conducting Polymer Solution and Gel Processing." *Reference Module in Materials Science and Materials Engineering,* Elsevier, 2017. https://doi.org/10.1016/B978-0-12-803581-8.03733-4.
15. Lanc, Z., Zeljković, M., Štrbac, B., Živković, A., Drstvenšek, I. & Hadžistević, M.. "The determination of the emissivity of aluminum alloy AW 6082 using infrared thermography." *J. Prod. Eng*, 18 (2015): 23-26.
16. Ranabhat, B. & Hsiao, K. T. "Improve the through-thickness electrical conductivity of CFRP laminate using flow-aligned carbon nanofiber z-threads". *Proceedings of SAMPE 2018*, Long Beach, CA, May 21-24, 2018.

17. Scruggs, M., Kirmse, S. & Hsiao, K.-T., “Enhancement of through-thickness thermal transport in unidirectional carbon fiber reinforced plastic laminates due to the synergetic role of carbon nanofiber z-threads.” *Journal of Nanomaterials*, Article ID 8928917 (2019): 13 pages, https://doi.org/10.1155/2019/8928917.

18. Loh, K. & Nagarajaiah, S. eds. *Innovative developments of advanced multifunctional nanocomposites in civil and structural engineering*". Woodhead Publishing, 2016.

19. McAndrew, T.P., Havel, M., Korzenko, A. & Delprat, P., “Composites with Multi-Walled Carbon Nanotubes.” NSTI-Nanotech 2013, www.nsti.org, ISBN 978-1-14822-0582-7, 1, 2013.